

# Dielectric characteristics of doped $\text{Ba}_{1-x}\text{Sr}_x\text{TiO}_3$ at the paraelectric state

J.W. Liou, B.S. Chiou \*

Department of Electronics Engineering and Institute of Electronics, National Chiao Tung University, Hsinchu 300, Taiwan, ROC

Received 25 November 1996; revised 30 April 1997; accepted 30 April 1997

## Abstract

$\text{Ba}_{1-x}\text{Sr}_x\text{TiO}_3$  ( $x=0$  to 1) ferroelectric ceramics doped with 1.0 mol.% MgO and 0.05 mol.%  $\text{MnO}_2$  were prepared with a rate-controlled sintering profile. The lattice constant of this BST system decreases as the strontium molar fraction increases. This is due to the smaller  $\text{Sr}^{2+}$  ionic radius than that of  $\text{Ba}^{2+}$ . The temperature dependence of the dielectric constant is measured at 10 kHz. A linear relation of the Curie temperature of the BST system to the Sr fraction for  $x \leq 0.75$  is observed. When this reaction is fitted to a modified Curie–Weiss law, two parameters, the critical exponent and the diffuseness parameter, which represent the order of transition broadening, can be calculated. From the values of these two parameters, it is suggested that the physical meanings of these two parameters are correlated to each other. The transition broadening is greatest for  $x=0.5$  owing to the most composition fluctuation. Dipole relaxation of the composition with  $x=0.25$  is observed at frequencies above 1 MHz. On the basis of Cole–Cole analysis, a low frequency relaxation due to dopants  $\text{Mn}^{2+}$  at below 50 kHz is observed. © 1997 Elsevier Science S.A.

**Keywords:** Dielectric characteristics; Ferroelectric material; Paraelectric state; Curie–Weiss law; Transition broadening

## 1. Introduction

Ferroelectric barium strontium titanate (BST) is of great interest for many practical applications. The Curie temperature of  $\text{Ba}_{1-x}\text{Sr}_x\text{TiO}_3$  ( $x=0$  to 1) can be controlled to meet the requirements of various applications by varying the strontium molar fraction  $x$ . Many experimental and theoretical studies have been performed on the dielectric properties of BST in the ferroelectric state [1–3]. However, little attention has been paid to the dielectric characteristics of the paraelectric state. The dielectric loss which is often important for dielectrics applications is usually lower in the paraelectric state than in the ferroelectric state owing to the disappearance of hysteresis.

The main purpose of this study is to investigate the effect of Sr ions substituting Ba sites on the dielectric properties of the paraelectric state for  $\text{MnO}_2$ - and MgO-doped  $\text{Ba}_{1-x}\text{Sr}_x\text{TiO}_3$  systems. The strontium molar fraction  $x$  was varied from 0 to 1 with an interval of 0.25 to adjust the Curie temperature of the BST system. Dopant  $\text{MnO}_2$  is used to trap the electrons to obtain low loss dielectrics [4], while dopant MgO serves as a grain growth inhibitor [5]. A nonisothermal

rate-controlled firing profile is employed to obtain uniform microstructure of the samples [5].

## 2. Experimental procedure

Doped  $\text{Ba}_{1-x}\text{Sr}_x\text{TiO}_3$  polycrystalline samples were prepared by a rate-controlled sintering profile. Commercial powders of  $\text{BaCO}_3$ ,  $\text{SrCO}_3$ ,  $\text{TiO}_2$ ,  $\text{MnO}_2$ , and MgO (Merck & Co., Inc., Darmstadt, Germany) together with acetone were ball milled with alumina balls for 24 h. An excess 1.0 mol.% of  $\text{TiO}_2$  was added to obtain a  $\text{TiO}_2$ -rich liquid phase during sintering [6]. The concentrations of MgO and  $\text{MnO}_2$  are 1.0 mol.% and 0.05 mol.%, respectively. After drying by IR lamp lighting, the mixture was calcined in an alumina crucible at 1100°C for 2 h in air. Sintering of samples was carried out with a controlled firing profile [4] after the binder had been burned out at 400°C for 3 h. This nonisothermal rate-controlled sintering profile has an initial heating rate of 100°C  $\text{min}^{-1}$  from 400°C to 1200°C, with a 6 min hold at 1200°C, and then up to a sintering temperature of 1400°C at the same heating rate. The sintering time was 18 min at 1400°C and then the samples were cooled to room temperature with a rate of  $-180^\circ\text{C h}^{-1}$ . The powders were then mixed with a small amount of PVA binder and pressed to form disk-shaped samples at 180 MPa. Phase identification

\* Corresponding author. Department of Electronics Engineering and Institute of Electronics, National Chiao Tung University, 1001 Ta Hseuh Rd., Hsinchu, 300, Taiwan. Fax: +886 3 572 4361, e-mail: 8211816@cc.nctu.edu.tw.

of these specimens was carried out with an X-ray powder diffractometer (Rigaku, Dmax-B, Japan) with Cu K $\alpha$  radiation. A scanning electron microscope (Hitachi, S570, Japan) was employed to examine the microstructures. The lattice constants were calculated based on the least-square refinement with over nine peaks of diffraction pattern. The average grain size was determined by the linear intercept method from the micrograph of the as-sintered sample. As-sintered samples in the disk shape were polished to 0.4 mm in thickness and electroded by rubbing In–Ga (40:60) alloy on both surfaces for providing ohmic contacts. The dielectric constant of each sample is calculated from the capacitance. The capacitance is measured with HP4192A LCR meters (Hewlett Packard) in the frequency range from 500 Hz to 4 MHz.

### 3. Results and discussion

The crystal structures obtained from the X-ray diffraction patterns are tetragonal phases for  $x=0$  and 0.25, and cubic phases for  $x=0.5$ , 0.75, and 1. Lattice parameter  $a$  decreases

Table 1  
The crystal structure, lattice constant, and the average grain size of the 1.0 mol.% MgO and 0.05 mol.% MnO<sub>2</sub> doped Ba<sub>1-x</sub>Sr<sub>x</sub>TiO<sub>3</sub> system

Sr molar fraction	Structure <sup>a</sup>	Lattice constant <sup>a</sup> (Å)	Average grain size (μm)
$x=0$	tetragonal	$c=4.032$ $a=3.994$	13.8
$x=0.25$	tetragonal	$c=3.992$ $a=3.980$	9.5
$x=0.5$	cubic	$a=3.960$	4.6
$x=0.75$	cubic	$a=3.931$	2.8
$x=1$	cubic	$a=3.905$	2.2

<sup>a</sup> At room temperature.

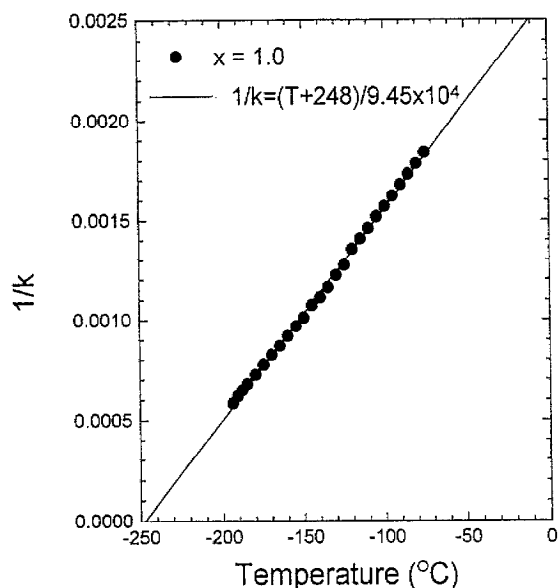


Fig. 1. Inverse of dielectric constant as function of temperature of doped SrTiO<sub>3</sub> at the paraelectric state.

from 3.994 Å for  $x=0$  (BaTiO<sub>3</sub>) to 3.905 Å for  $x=1$  (SrTiO<sub>3</sub>). The decrease in lattice constants is attributed to the smaller Sr<sup>2+</sup> ionic radius ( $\approx 1.16$  Å) than that of Ba<sup>2+</sup> ( $\approx 1.36$  Å) [7]. Scanning electron micrographs on the bulk surfaces reveal a decrease of grain size from 13.8 μm to 2.2 μm as the Sr molar fraction  $x$  is raised from 0 to 1. It seems that MgO additive is more effective in inhibiting the grain growth for Sr-rich composition. The crystal structure, the lattice constants and the average grain size for the doped BST system with different Sr molar fraction are listed in Table 1.

The temperature dependence of the reciprocal of the dielectric constant of SrTiO<sub>3</sub> in the paraelectric state is shown in Fig. 1 where the dielectric behaviour follows the Curie–Weiss law. The Curie temperature of doped SrTiO<sub>3</sub> is beyond the temperature range ( $-190^{\circ}\text{C}$  to  $150^{\circ}\text{C}$ ) of the experimental apparatus. The hypothetical Curie temperature  $T_C$  of SrTiO<sub>3</sub> is estimated to be at  $-248^{\circ}\text{C}$  by the theoretical fitting with Curie–Weiss law, i.e.  $1/k=(T-T_C)/C$ . The Curie constant  $C$  is about  $9.45 \times 10^4$  °C. The Curie temperatures together with the maximum dielectric constants for the doped BST system are listed in Table 2. Although the Sr-rich specimen had a smaller grain size, the maximum dielectric constant increases as the Sr molar fraction increases from 0.25 to 0.75. It has been reported that internal stress in the grains reduces the maximum dielectric constant of barium titanate and that smaller grains have higher internal stress [8,9]. It seems that the grain size effect does not dominate the dielectric properties of Sr-rich samples. The  $T_C$  values for BaTiO<sub>3</sub> and SrTiO<sub>3</sub> in this study are  $104^{\circ}\text{C}$  and  $-248^{\circ}\text{C}$  respectively. They are lower than literature-reported data for undoped BaTiO<sub>3</sub> ( $T_C \approx 128^{\circ}\text{C}$ ) and SrTiO<sub>3</sub> ( $T_C \approx -233^{\circ}\text{C}$ ) [4,8,9]. It is believed that Mn dopant causes the lowering of  $T_C$ . The Mn<sup>2+</sup> ions, which occupy the Ti<sup>4+</sup> ion sites, result in oxygen vacancies and lead to a ‘break’ of the cooperative vibration of the TiO chains, and, consequently shift the Mn-doped system to lower  $T_C$  [4].

Effects of Sr molar fraction on the lattice constant and Curie temperature for the doped BST system are presented in Fig. 2. Substituting of the smaller ions of Sr<sup>2+</sup> on Ba<sup>2+</sup> sites is believed to decrease the lattice constant and the Curie

Table 2  
The Curie temperature and the maximum dielectric constant of the 1.0 mol.% MgO and 0.05 mol.% MnO<sub>2</sub> doped Ba<sub>1-x</sub>Sr<sub>x</sub>TiO<sub>3</sub> system

Sr molar fraction	Curie temperature $T_C$ (°C)	Maximum dielectric constant $k_{\text{max}}$
$x=0$	$104^{\circ}\text{C}$	9837
$x=0.25$	$34^{\circ}\text{C}$	8744
$x=0.5$	$-40^{\circ}\text{C}$	10315
$x=0.75$	$-132^{\circ}\text{C}$	11770
$x=1$	$-248^{\circ}\text{C}^{\text{a}}$	<sup>a</sup>

<sup>a</sup>  $T_C$  for  $x=1$  is estimated from the fitting of Curie–Weiss law in Fig. 1 and the  $k_{\text{max}}$  for  $x=1$  is not measured.

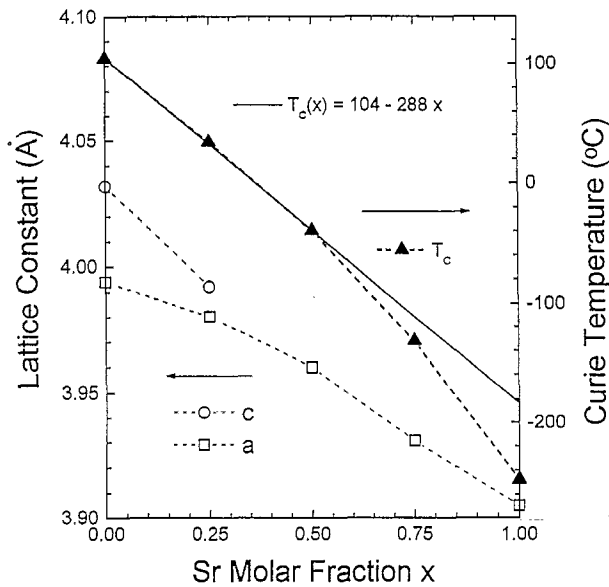


Fig. 2. Lattice constants and the Curie temperature as function of Sr molar fraction for doped  $Ba_{1-x}Sr_xTiO_3$  system.

temperature. A feature to be noted is that the Curie temperature is linearly related to the Sr molar fraction for  $x \leq 0.5$ , while for specimens of  $x = 0.75$  and  $x = 1$ , deviation from this linearity is observed. Viana et. al. [10] reported that the ferroelectric transition temperature ( $T_C$ ) of pure  $SrTiO_3$  was 40 K which was lower than the structural phase transition temperature at 105 K. They suggested that the reduction of  $T_C$  is caused by the suppression of long-range ferroelectric order by the quantum fluctuation at low temperatures. It is argued that the deviation of the Curie temperature for compositions  $x = 0.75$  and  $x = 1$  from linearity (Fig. 2) also results from the suppression of long-range ferroelectric order.

The temperature dependence of dielectric constant at the paraelectric state can be fitted by a modified Curie–Weiss law [11]:

$$\frac{1}{k} = \frac{1}{k_{max}} \left[ 1 + \frac{(T - T_C)^\gamma}{\delta} \right] \quad (1)$$

where  $T_C$  is the Curie temperature at maximum dielectric constant  $k_{max}$ , and  $\gamma$  and  $\delta$  are the critical exponent and diffuseness parameter, respectively. This empirical equation is derived on the basis of a Gaussian distribution of the Curie temperatures. It is noted that the physical meanings of  $\gamma$  and  $\delta$  are correlated to each other and represent the order of the transition broadening. As the critical exponent  $\gamma$  obtained from the experimental data increases, the diffuseness parameter  $\delta$  also increases to keep the ratio,  $(T - T_C)^\gamma/\delta$ , in a reasonable range. Fig. 3 gives  $k_{max}/k - 1$  versus  $T - T_C$  curves for specimens of  $x = 0$  to 0.75. The experimental results fit well with the theoretical curve of the modified Curie–Weiss law. Parameters  $\gamma$  and  $\delta$  for each composition of BST system are shown in Fig. 4. Similar trends of these two parameters are observed, presumably because they have similar physical meanings. Both the critical exponents and the diffuseness parameters show maxima at  $x = 0.5$ . Two possible factors may increase the critical exponent and the diffuseness parameter. Firstly, for samples with smaller grains, the internal stress plays a more important role [8,9,12] to diffuse the transition. Thus, temperature dependence of dielectric constant shows large  $\gamma$  and  $\delta$ . Secondly, fluctuation in composition of a ferroelectric material, such as the Ba to Sr ratio in  $(Ba,Sr)TiO_3$ , may lead to a distribution of Curie temperatures in a single sample [13]. Hence the diffuseness of the transition is observed. In this study, the grain size of  $Ba_{1-x}Sr_xTiO_3$  decreases from 13.8  $\mu m$  to 2.2  $\mu m$  as the Sr molar fraction increases from 0 to 1. Previous works [8,9] showed that the internal stress due to the grain size effect is only significant for fine grained (less than 1  $\mu m$ ) samples. It is plausible that the grain size effect does not dominate in this  $Ba_{1-x}Sr_xTiO_3$  system. Besides, the probability of compositional fluctuation

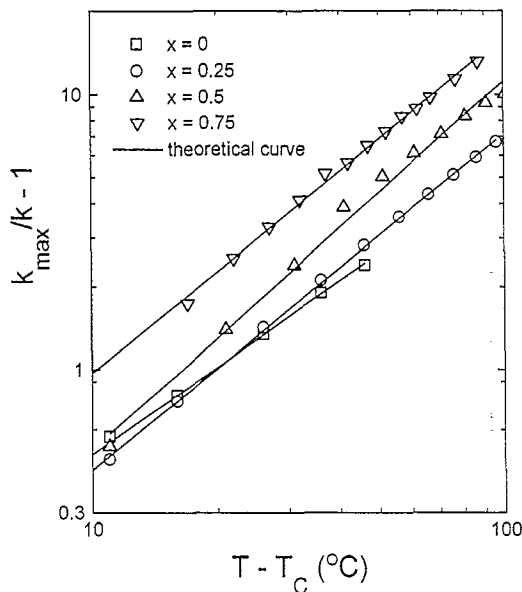


Fig. 3.  $k_{max}/k - 1$  vs.  $T - T_C$  for doped  $Ba_{1-x}Sr_xTiO_3$ . The solid lines are the theoretical curve based on the modified Curie–Weiss law.

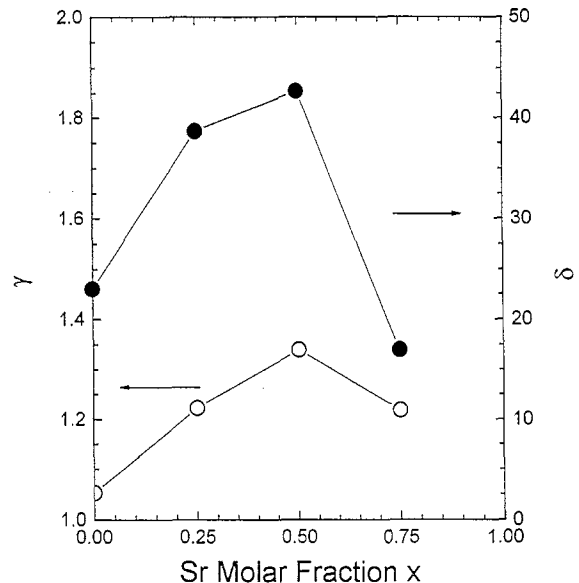


Fig. 4.  $\gamma$  and  $\delta$  as function of Sr molar fraction for doped  $Ba_{1-x}Sr_xTiO_3$ . The values of them are obtained from the fittings in Fig. 3.

in a system containing two phases of ferroelectric solid solution is largest when the concentrations of both phases are equal. Therefore, maxima of  $\gamma$  and  $\delta$  at  $x=0.5$  are believed to be mostly due to the compositional fluctuation in samples. Compositional fluctuation has been reported in previous works by Chiou, Ganesh and Goo [14–16]; it results in the flattening of dielectric peak and the broadening of dielectric transition.

The frequency dependence of the dielectric constant and dielectric loss at various temperatures for the specimen of  $x=0.25$  are shown in Figs. 5 and 6, respectively. The decrease in dielectric constant is apparent at frequencies greater than 1 MHz where an abrupt increase in dielectric loss is observed. The dipolar relaxation in the perovskite structure of  $\text{Ba}_{0.75}\text{Sr}_{0.25}\text{TiO}_3$  is observed here. The Cole–Cole expression is employed to analyse the dielectric dispersion:

$$\varepsilon(\omega) = \varepsilon_{\infty} + \frac{\varepsilon_0 - \varepsilon_{\infty}}{1 + (i\omega\tau)^{1-\alpha}} \quad (2)$$

where  $\omega$  and  $\tau$  are the response frequency and the relaxation time of dipole interactions,  $\varepsilon_0$  and  $\varepsilon_{\infty}$  are the static and optical relative permittivities, respectively. The tilt parameter  $\alpha$  denotes an order of broad distribution of relaxation time thus  $\tau$  is a measure of the global average relaxation time. The complex relative permittivity  $\varepsilon(\omega)$  can be written in the form:

$$\varepsilon(\omega) = \varepsilon'(\omega) - j\varepsilon''(\omega) \quad (3)$$

The dielectric constant is by definition the real part of the relative permittivity  $\varepsilon'$ . The imaginary part of relative permittivity  $\varepsilon''$  can be obtained by the product of dielectric constant and the dielectric loss, i.e.  $\varepsilon'' = \varepsilon' \tan \delta$ . On the basis of

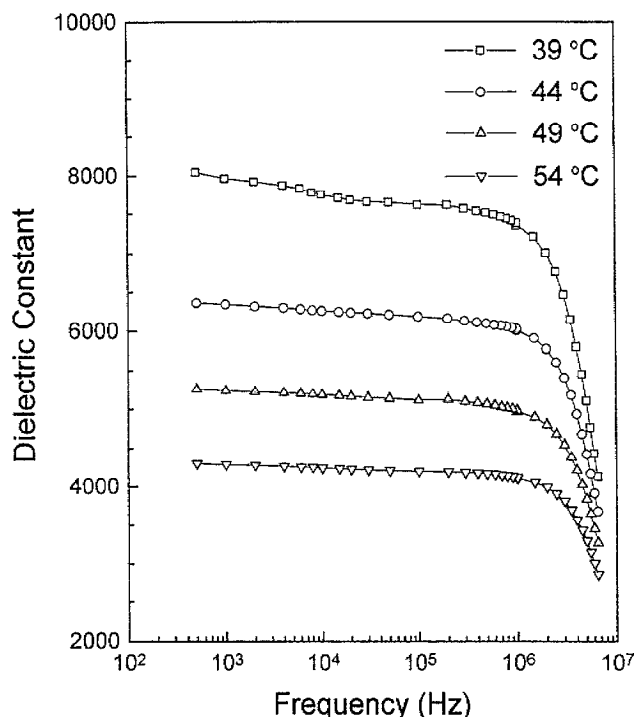


Fig. 5. Frequency dependence of dielectric constant for the sample  $x=0.25$  ( $T_C \approx 34^\circ\text{C}$ ) at various temperature.

data given in Figs. 5 and 6, Cole–Cole plot of  $\varepsilon'$  versus  $\varepsilon''$  are shown in Fig. 7. The solid lines in Fig. 7, obtained with Eq. (2), fit well with the experimental data except at low frequency. At frequencies below 50 kHz, the dielectric losses are higher than those predicted by the Cole–Cole equation. Dopant  $\text{MnO}_2$  is believed to contribute to the high dielectric loss at low frequencies. It was reported by Iguchi and Lee [17] that two relaxation mechanisms were found at several tens of kHz for doped  $\text{SrTiO}_3$  in the paraelectric state. They argued that the dopants they employed,  $\text{La}_2\text{O}_3$  and  $\text{MnO}_2$ , caused a two-relaxation phenomenon, since  $\text{La}^{3+}$  and  $\text{Mn}^{4+}$  ions substituted  $\text{Ti}^{4+}$  sites and produced more than one off-centre equilibrium position of  $\text{Ti}^{4+}$ .

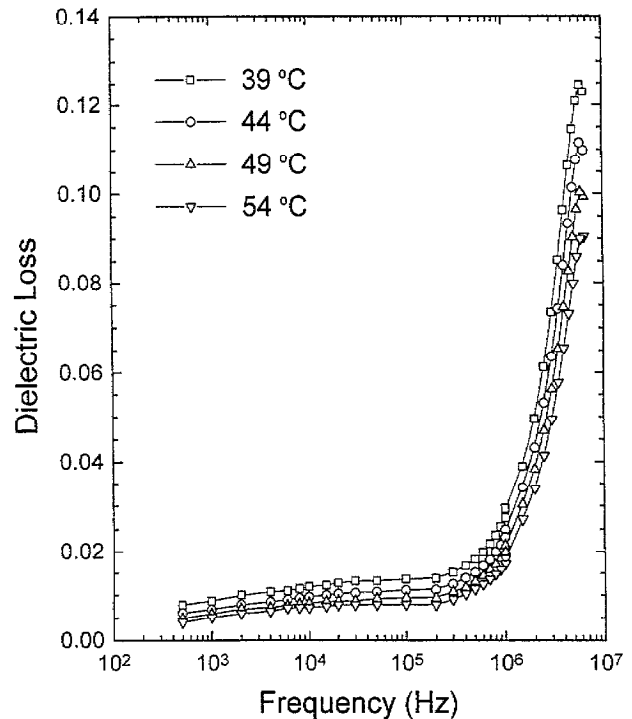


Fig. 6. Frequency dependence of dielectric loss of the sample  $x=0.25$  ( $T_C \approx 34^\circ\text{C}$ ) at various temperature.

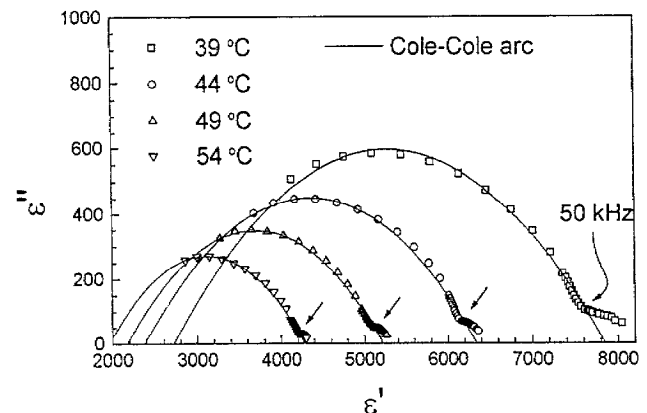


Fig. 7. Cole–Cole plot of the relative permittivities  $\varepsilon'$  vs.  $\varepsilon''$  for the sample  $x=0.25$  ( $T_C \approx 34^\circ\text{C}$ ) at various temperature. The solid lines are the fitted Cole–Cole arcs. The arrows indicate the higher loss than that predicted by Cole–Cole arcs at frequencies below 50 kHz.

Table 3

Static relative permittivity  $\epsilon_0$ , optical relative permittivity  $\epsilon_\infty$ , global average relaxation time  $\tau$ , and tilt parameter  $\alpha$  obtained from the Cole–Cole expression for 1.0 mol.% MgO and 0.05 mol.% MnO<sub>2</sub> doped Ba<sub>0.75</sub>Sr<sub>0.25</sub>TiO<sub>3</sub> at four different temperatures

Temperature (°C)	$\epsilon_0$	$\epsilon_\infty$	$\tau$ ( $\times 10^{-7}$ s)	$\alpha$
39	7845	2718	2.27	0.708
44	6340	2375	2.08	0.714
49	5219	2170	1.95	0.712
54	4277	1958	1.88	0.707

On the basis of the Cole–Cole arc shown in Fig. 7, the static and optical relative permittivities together with global average relaxation time and tilt parameter at different temperatures are obtained and summarized in Table 3. Both static and optical permittivities decrease with the increase of temperature following the Curie–Weiss behaviour. The tilt parameters of around 0.71 suggest a broad distribution of relaxation times. The temperature independence of these values indicates that thermal energies do not influence the distribution of relaxation times. However, high temperature provides enough thermal energy to decrease the global relaxation time. The activation energy  $E_a$  for this dipole relaxation can be obtained by exponentially temperature dependent of relaxation time, i.e.,  $\tau = \tau_0 \exp(E_a/kT)$ . For Ba<sub>0.75</sub>Sr<sub>0.25</sub>TiO<sub>3</sub> ( $x = 0.25$ ), the activation energy  $E_a$  and intrinsic relaxation time  $\tau_0$  obtained from the data listed in Table 3 are about 0.11 eV is about 3.49 ns, respectively.

#### 4. Conclusions

(1) The dielectric behaviour of the Ba<sub>1-x</sub>Sr<sub>x</sub>TiO<sub>3</sub> system doped with 1.0 mol.% MgO and 0.05 mol.% MnO<sub>2</sub> was investigated. In the paraelectric state, the dielectric constant of doped Ba<sub>1-x</sub>Sr<sub>x</sub>TiO<sub>3</sub> follows the modified Curie–Weiss law.

(2) Grain size and compositional fluctuation are two major factors affecting the broadening of ferroelectric to paraelectric transition for this doped Ba<sub>1-x</sub>Sr<sub>x</sub>TiO<sub>3</sub> system.

(3) Dipolar relaxation of doped Ba<sub>0.75</sub>Sr<sub>0.25</sub>TiO<sub>3</sub> is observed at frequencies around 1 MHz. This dispersion spectrum can be analysed by Cole–Cole expression. Another dielectric relaxation due to dopant Mn<sup>4+</sup> is observed at below 50 kHz.

(4) The independence of the tilt parameter from temperature for doped Ba<sub>0.75</sub>Sr<sub>0.25</sub>TiO<sub>3</sub> in the paraelectric state suggests that thermal energy affects the global average relaxation time rather than the distribution of relaxation time.

#### Acknowledgements

This work is supported by the Chung-Shan Institute of Science and Technology (contract No. CS 85-0210-D-009-009) and partly supported by the National Science Council of Taiwan, ROC (contract No. NSC 86-2623-D-009-002).

#### References

- [1] U. Syamaprasad, R.K. Galgali and B.C. Mohanty, *Mater. Lett.*, 7 (5–6) (1988) 197.
- [2] B.S. Chiou and S.T. Lin, *Mater. Chem. Phys.*, 20 (1988) 431.
- [3] F.S. Yen, H.I. Hsiang and Y.H. Chang, *Jpn. J. Appl. Phys.*, 34 (11) (1995) 6149.
- [4] F. Batllo, E. Duverger, J.C. Niepce, B. Janot and M. Maglione, *Ferroelectrics*, 109 (1990) 113.
- [5] B.S. Chiou, C.M. Koh and J.G. Duh, *J. Mater. Sci.*, 22 (1987) 3893.
- [6] H.U. Anderson, *J. Am. Ceram. Soc.*, 56 (11) (1973) 605.
- [7] S.B. Herner, F.A. Selmi, V.V. Varadan and V.K. Varadan, *Mater. Lett.*, 15 (1993) 317.
- [8] G. Arlt, D. Hennings and G. de With, *J. Appl. Phys.*, 58 (4) (1985) 1619.
- [9] T.T. Fang, H.L. Hsieh and F.S. Shiau, *J. Am. Ceram. Soc.*, 76 (5) (1993) 1205.
- [10] R. Viana, P. Lunkenheimer, J. Hemberger, R. Böhmer and A. Loidl, *Phys. Rev. B*, 50 (1994) 601.
- [11] K. Uchino and S. Nomura, *Ferroelectrics*, 44 (1982) 55.
- [12] H.T. Martirena and J.C. Burfoot, *J. Phys. C*, 7 (1974) 3182.
- [13] B.N. Rolov, *Sov. Phys. Solid State*, 6 (7) (1965) 1676.
- [14] R. Ganesh and E. Goo, *J. Am. Ceram. Soc.*, 79 (1996) 225.
- [15] B.S. Chiou and R.W. Vest, *Bull. Am. Ceram. Soc.*, 63 (1984) 811.
- [16] B.S. Chiou, *IEEE Trans. Comp., Hybrid and Manu. Tech.*, 12 (1989) 798.
- [17] E. Iguchi and K.J. Lee, *J. Mater. Sci.*, 28 (1993) 5809.